

INSTITUTE FOR FUSION STUDIES

DOE/ET-53088-578

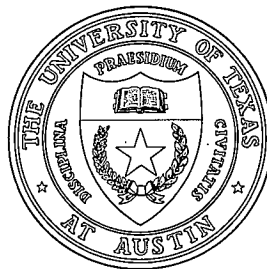
IFSR #578

Kinetic Theory of Toroidicity and
Ellipticity-Induced Alfvén Eigenmodes

R.R. METT and S.M. MAHAJAN
Institute for Fusion Studies
The University of Texas at Austin
Austin, Texas 78712

October 1992

THE UNIVERSITY OF TEXAS



AUSTIN

Kinetic Theory of Toroidicity and Ellipticity-Induced Alfvén Eigenmodes

R.R. Mett and S.M. Mahajan
Institute for Fusion Studies
The University of Texas at Austin
Austin, Texas 78712

Abstract

A recent non-perturbative kinetic analysis of the toroidicity induced Alfvén eigenmode (TAE) has shown that electron parallel dynamics can strongly influence their character and damping.¹ The TAE was demonstrated to have a large damping, for a large range of parameters, because of a merging of the mode structure with the kinetic Alfvén wave (KAW) within the gap region. In this non-perturbative regime, the damping is relatively insensitive to the dissipative mechanisms because the KAW carries the mode energy away from the gap region. The theory also predicted a new mode, a kinetic TAE (KTAE), which is formed by the toroidal coupling of two KAW's. In the present study, we extend the analysis to the ellipticity induced Alfvén eigenmode (EAE). We find that the parameter which measures the kinetic character of the EAE is significantly smaller than it is for the TAE for elongated plasmas like DIII-D. Consequently, the parameter is rather small for the lower mode number EAE's but it becomes of order unity or larger for the higher mode numbers because the parameter scales as the square of the mode number. It is therefore highly desirable to have an analytic description of the transition from the perturbative to the non-perturbative regimes. The present study presents such a theory and also examines the kinetic EAE

(KEAE) in further detail. Quite significantly, the transition to the non-perturbative regime can begin for very small values of the kinetic parameter.

To appear in "Theory of Fusion Plasmas," *Proceedings of the Joint Varenna-Lausanne International Workshop, Varenna, Italy, 1992* (Editorie Compositori Societa Italiana di Fisica, Bologna, 1993).

I. Introduction

Toroidicity-induced Alfvén eigenmodes (TAE) and ellipticity-induced Alfvén eigenmodes (EAE) are currently of great interest because they may destroy the confinement of fast ions in a burning tokamak plasma.²⁻¹³ Their excitation depends on the difference between the growth rate due to the fast ions and the damping rate, mainly due to electrons. Initial theories have predicted very low intrinsic damping for TAE, and a significant fast ion drive.^{3,4} However, experiments with beam-driven TAE^{6,7} suggest an excitation threshold at least an order of magnitude higher than these initial theories predicted. More recent theoretical studies have indicated that alternate damping mechanisms, such as continuum damping,⁸⁻¹¹ trapped electron effects,¹² and kinetic effects,¹ are important. The present study focuses on the latter, extending the non-perturbative kinetic analysis of the TAE to the EAE.

We find that the parameter which measures the kinetic character of the EAE is significantly smaller than it is for the TAE for elongated plasmas like DIII-D. The parameter is rather small for the lower mode numbers but attains values of order unity or larger for the higher mode numbers, since the parameter scales as the square of the mode number. Consequently, one expects the lower mode number EAE's to have a strongly magnetohydrodynamic (MHD) character, and to suffer only perturbative damping that depends linearly on the dissipative mechanisms. However, while the former is true, the latter is not necessarily the case. Quite significantly, the transition to the non-perturbative regime can begin for very small values of the kinetic parameter. In the non-perturbative regime, the damping is enhanced because of a merging of the mode structure with the kinetic Alfvén wave (KAW) within the gap region. The damping is relatively insensitive to the dissipative mechanisms because the KAW carries the mode energy away from the gap region. In addition to altering the mode structure, kinetic effects introduce a countable infinity of new modes, formed by

the coupling between two erstwhile KAW's. These kinetic T/EAE (KT/EAE) have eigenfrequencies which lie just above the gap. The lowest KT/EAE may actually have a lower damping rate than the corresponding T/EAE due to non-perturbative effects. This makes the KT/EAE potentially more important than the T/EAE under some conditions. The present work examines these kinetic T/EAE (KT/EAE) in further detail.

II. Basic Equations

Betti and Freidberg⁵ have studied the EAE in ideal MHD when ellipticity can be treated as a perturbation and the effect of toroidicity can be neglected with respect to the ellipticity. In this limit, the flux coordinates (r', θ') are expressed as perturbations of cylindrical coordinates (r, θ) ,

$$r' = r - \xi(r) \cos 2\theta , \quad (1a)$$

$$\theta' = \theta + f(r) \sin 2\theta . \quad (1b)$$

Here, $\xi(r)$ represents the elliptical distortion and $f(r)$ is related to $\xi(r)$ through the particular choice of flux coordinates. Betti and Freidberg show that $\xi(r)$ is governed by a perturbed Grad-Shafranov equation. To a good approximation, $\xi = -r(\chi - 1)/2$, where χ is the elongation of the plasma ($\chi \sim 1.6$ for DIII-D). For symmetry coordinates, it is possible to prove that

$$f(r) = (\xi/r + d\xi/dr)/2 , \quad (2)$$

because the safety factor q is a flux function and therefore independent of θ' . For a general discussion of symmetry coordinates, see e.g. Hazeltine and Meiss.¹³ [We point out that Betti and Freidberg incorrectly use $f(r) = \xi/r$. Despite this, their final equation, Eq. (23), is correct because they keep only the coupling terms with the highest radial derivatives.] The simplified gap mode equation is derived from an equation for Alfvén waves in general geometry [e.g. Eq. (10) of Betti and Freidberg] by expressing the differential operators

in terms of (r', θ') . One can see from Eqs. (1a) and (1b) that ellipticity couples poloidal harmonics that differ by 2.

With electron parallel dynamics, the simplified gap mode equation may be written (dropping the primes from the flux coordinates),

$$\begin{aligned} & \left[r K_1^2 \frac{d}{dr} \frac{\Delta_1}{r K_1^2} \frac{d}{dr} r - r K_1^2 (\Delta_1 - G_1) \right. \\ & \quad \left. + K_1 k_1 \left(\frac{d}{dr} r \frac{d}{dr} - r K_1^2 \right) \frac{\tau_1}{K_1 k_1} \left(\frac{1}{r^2} \frac{d}{dr} r \frac{d}{dr} r - K_1^2 \right) \right] E_1 \\ & = -2 \left(\frac{1}{r} \frac{d}{dr} \varepsilon r \frac{\omega^2}{v_A^2} \frac{d}{dr} + K_1 K_2 \varepsilon \frac{\omega^2}{v_A^2} \right) r E_2, \end{aligned} \quad (3)$$

where the subscripts 1 and 2 designate quantities associated with the poloidal harmonics m_1 and m_2 , respectively. In this equation, the poloidal electric field $E(r) \sim e^{i(m\theta - n\phi - \omega t)}$, the poloidal wavenumber $K = m/r$, the parallel wavenumber $k = (m/q - n)/R$, the coupling strength $\varepsilon(r) = -d\xi(r)/dr$, while $\Delta = \omega^2/v_A^2 - k^2$, $G = (dk^2/dr)/(rK^2)$ is proportional to the shear and contains the effect of equilibrium current, and τ measures the effect of electron parallel dynamics (parallel electric field). It is related to the parallel conductivity σ as $\tau = -i\omega/(\sigma\mu_0 v_A^2)$. We point out that all shear-dependent and τ -dependent coupling terms have been dropped from Eq. (3) for simplicity. Unlike many other authors, we retain the K -dependent coupling terms.

One may notice that the simplified gap mode equation for the TAE (neglecting elliptical distortion) is very similar,¹ with only a minor change in the coupling term. For the TAE, ε in Eq. (3) is replaced by the inverse aspect ratio r/R ($1.25r/R$ if a Shafranov shift in the equilibrium is included) and $K_1 K_2$ is replaced by $-K_2^2$. The coupling terms for the TAE are generated by the operator $\mathbf{B} \cdot \nabla$, from the variation of B and R with θ through $R = R_0(1 + \varepsilon \cos \theta)$. For the EAE, the coupling terms are generated by ∇_\perp^2 .

Without electron inertia or coupling, Eq. (3) is singular where $\Delta(r) = 0$, which defines

the location of the Alfvén continuum. Here, $E \sim \ell n(\Delta)$. Coupling introduces gaps in the continuum near the radial position where $\Delta_1 = \Delta_2$, or equivalently $k_1 = -k_2$. The continua are defined by

$$\begin{pmatrix} \Delta_1 & 2\varepsilon \frac{\omega^2}{v_A^2} & 0 & \cdots \\ 2\varepsilon \frac{\omega^2}{v_A^2} & \Delta_2 & 2\varepsilon \frac{\omega^2}{v_A^2} & \cdots \\ 0 & 2\varepsilon \frac{\omega^2}{v_A^2} & \Delta_3 & \cdots \\ \cdots & \cdots & \cdots & \cdots \end{pmatrix} \begin{pmatrix} E_1'' \\ E_2'' \\ E_3'' \\ \cdots \end{pmatrix} = 0. \quad (4)$$

Whereas for the TAE $|k| = 1/(2qR)$, for the EAE $|k| = 1/(qR)$. Electron inertia (and FLR), by making system higher order, resolves the continuum and introduces the kinetic Alfvén wave (KAW).^{14,15} The KAW is radially propagating and is usually strongly damped.

Our parallel conductivity model includes collisionless (Landau) damping on passing electrons and collisional damping on both trapped and passing electrons. We find $\tau = k^2 \rho_s^2 / F$, where $\rho_s = c_s / \omega_{ci}$ and F is a complicated function whose details are given in Ref. 1. Typically, F is near unity. For the collisionless case, the trapped particles tend to decrease the imaginary part of F to a small fraction of the real part, which remains nearly unity. Collisions have their largest effect on the imaginary part of F , increasing it to a significant fraction of the real part for typical plasma parameters.

We focus on the mode structure near a single gap and assume that the mode energy falls off rapidly outside this region. The coupled system is then completed with the equation formed by exchanging the subscripts $1 \leftrightarrow 2$. Following the analysis of Ref. 1, we take Eq. (3) and its counterpart and make the same expansion in slab geometry [$\phi(r) \equiv rE(r)$, $r = r_o + x$, $\Delta_1 = \Delta - \alpha_1 x$, $\Delta_2 = \Delta + \alpha_2 x$, where $\alpha_1 = -d\Delta_1/dr|_{r_o}$, $\alpha_2 = d\Delta_2/dr|_{r_o}$], take the Fourier transform [$\phi(x) = \int_{-\infty}^{\infty} dp \tilde{\phi}(p) e^{ipx}$], and symmetrize [$\psi_1 = \tilde{\phi}_1 [\alpha_1 e^{i\eta}(p^2 + K_1^2)]^{1/2}$, $\psi_2 = \tilde{\phi}_2 [\alpha_2 e^{i\eta}(p^2 + K_2^2)]^{1/2}$, where $\eta = (\alpha_1^{-1} - \alpha_2^{-1}) \times (\Delta p - \frac{1}{3} \tau p^3 (K_1^2/\alpha_1 - K_2^2/\alpha_2) p -$

$K_1 G_1 \alpha_1^{-1} \operatorname{atan}(p/K_1) + K_2 G_2 \alpha_2^{-1} \operatorname{atan}(p/K_2)]$. This leads to the coupled system

$$\left[\frac{d}{dy} + ih(y) \right] \psi_1 = -i\hat{\varepsilon} \psi_2 f(y), \quad (5a)$$

$$\left[\frac{d}{dy} - ih(y) \right] \psi_2 = i\hat{\varepsilon} \psi_1 f(y), \quad (5b)$$

where the normalized Fourier coordinate $y = p/\kappa$, the normalized inverse aspect ratio $\hat{\varepsilon} = 2\varepsilon\kappa(\alpha_1\alpha_2)^{-1/2}\omega^2/v_A^2$, while the functions $h(y) = \hat{\Delta} - \hat{G}(y) - \hat{\tau}(y^2 + 1)$, and $f(y) = (y^2 - y_1 y_2)/[(y^2 + y_1^2)(y^2 + y_2^2)]^{1/2}$. Here, the normalized eigenvalue $\hat{\Delta} = \frac{1}{2}\kappa\Delta/\alpha$, the normalized “shear” parameter $\hat{G}(y) = \frac{1}{2}[\hat{G}_1/(1 + y^2/y_1^2) + \hat{G}_2/(1 + y^2/y_2^2)]$, and the normalized inverse parallel conductivity $\hat{\tau} = \frac{1}{2}\tau\kappa^3/\alpha$, where $\kappa = [\alpha(K_1^2/\alpha_1 + K_2^2/\alpha_2)]^{1/2}$, $\alpha = (\alpha_1^{-1} + \alpha_2^{-1})^{-1}$, $\hat{G}_1 = \kappa G_1/\alpha_1$, $\hat{G}_2 = \kappa G_2/\alpha_2$, $y_1 = K_1/\kappa$, and $y_2 = K_2/\kappa$. The quantities Δ , τ , ε , v_A , K_1 , K_2 , G_1 , G_2 are all evaluated at $r = r_o$ and are therefore constants. The problem is reduced to a coupled pair of linear, first order, ordinary differential equations with the eigenvalue ω entering through $\hat{\Delta}(\omega)$, $\hat{\tau}(\omega)$, and $\hat{\varepsilon}(\omega)$. We put $\hat{\tau}(\omega) = \hat{\tau}(kv_A)$ and $\hat{\varepsilon}(\omega) = \hat{\varepsilon}(kv_A)$ and treat $\hat{\Delta}$ as the eigenvalue.

The analogous equations for the TAE [Eqs. (11a) and (11b) of Ref. 1] read

$$\left[\frac{d}{dy} + ih(y) \right] \psi_1 = -i\hat{\varepsilon} \psi_2 f(y), \quad (6a)$$

$$\left[\frac{d}{dy} - ih(y) \right] \psi_2 = \frac{i\hat{\varepsilon} \psi_1}{f(y)}, \quad (6b)$$

where now $f(y) = [(y^2 + y_2^2)/(y^2 + y_1^2)]^{1/2}$. Aside from the definition of ε , the only difference between these and Eqs. (5a) and (5b) is the form of $f(y)$ and the way in which it enters the problem.

In terms of the normalized variables, the eigenfrequency is given by

$$\omega = kv_A \left[1 + 4\varepsilon \frac{(m_1 m_2)^{1/2}}{m_1 + m_2} (\hat{\Delta}/\hat{\varepsilon}) \right]^{1/2}, \quad (7)$$

and so the damping is, to leading order in ε ,

$$\frac{\gamma}{\omega} = 2\varepsilon \frac{(m_1 m_2)^{1/2}}{m_1 + m_2} \operatorname{Im}(\hat{\Delta}/\hat{\varepsilon}), \quad (8)$$

and the gap boundary is determined by

$$\hat{\Delta}_{\text{gap}} = \pm \hat{\varepsilon} \frac{m_1 + m_2}{2(m_1 m_2)^{1/2}} . \quad (9)$$

III. Analytic Dispersion Relations

Significant simplification of Eqs. (5a) and (5b) can be made by transforming to a new coordinate $z = \hat{\varepsilon}y$. Then

$$\hat{\varepsilon}^{-1}h(z) \cong \Delta - G\delta(z) , \quad (10)$$

where $\Delta = \hat{\Delta}/\hat{\varepsilon}$, $G = \pi(\hat{G}_1 y_1 + \hat{G}_2 y_2)/2$, and we have approximated $\pi\delta(z) \cong \hat{\varepsilon}y_1/[z^2 + (\hat{\varepsilon}y_1)^2] \cong \hat{\varepsilon}y_2/[z^2 + (\hat{\varepsilon}y_2)^2]$. In a similar manner, we can write

$$f(z) \cong 1 - H\delta(z) , \quad (11)$$

where $H = 2\pi\hat{\varepsilon}(y_1 y_2)^{1/2}$. Substituting these into Eqs. (5a) and (5b), we find

$$\left[\frac{d}{dz} + i(\Delta - \tau z^2) \right] \psi_1 = -i\psi_2 + i[G\psi_1(0) + H\psi_2(0)]\delta(z) , \quad (12a)$$

$$\left[\frac{d}{dz} - i(\Delta - \tau z^2) \right] \psi_2 = i\psi_1 - i[G\psi_2(0) + H\psi_1(0)]\delta(z) , \quad (12b)$$

where $\tau = \hat{\tau}/\hat{\varepsilon}^3$. For the TAE problem, it is a good approximation to put $H = 0$, because of the way $f(z)$ appears in Eqs. (6a) and (6b).¹ Consequently, Eqs. (12a) and (12b) apply to both TAE and EAE.

We point out that Eqs. (12a) and (12b) are very similar to ones reported by M. N. Rosenbluth, J. Candy, H.L. Berk, J.W. Van Dam, and D.M. Lindberg, poster 3C38, at the 1992 International Sherwood Theory Conference, Santa Fe, NM, April 1992. Their equations are reproduced with the replacements $\Delta \rightarrow g_m$, $\tau \rightarrow a$, $\psi_2 \rightarrow \psi_m$, $\psi_1 \rightarrow \psi_{m-1}$, $[G\psi_2(0) + H\psi_1(0)] \rightarrow C_m$ and $[G\psi_1(0) + H\psi_2(0)] \rightarrow -C_{m-1}$, where the C 's represent the "fluxes," originally defined in Ref. 11 used in Refs. 9 and 10. Their theory can connect multiple gaps and the C 's represent asymptotic boundary conditions on the wave functions

far away from the gap. The C 's determine how the modes at each gap interact with one another. Since our problem is local, with the particular purpose of demonstrating the critical role of kinetics, we do not account for such interaction. Ours is a self-contained eigenvalue problem.

Due to symmetry, Eqs. (12a) and (12b) admit only solutions of the form

$$\psi_2(z) = \psi_1(-z) , \quad (13a)$$

or

$$\psi_2(z) = -\psi_1(-z) . \quad (13b)$$

We call solutions satisfying Eq. (13a) Type 1 solutions and those satisfying Eq. (13b) Type 2 solutions. Such symmetry suggests the construction of the symmetric and antisymmetric wave functions, $\psi_s(z) = \psi_1(z) + \psi_1(-z)$ and $\psi_a(z) = \psi_1(z) - \psi_1(-z)$. Equations (12a) and (12b) may be combined, for Type 1 solutions, into

$$\frac{d}{dz} \left[\frac{1}{1 - \Delta + \tau z^2} \frac{d\psi_s}{dz} \right] - [1 + \Delta - \tau z^2] \psi_s = -(G + H) \delta(z) \psi_s(0) . \quad (14)$$

For Type 2 solutions, we obtain Eq. (14) with the replacements $(\Delta, \tau, G) \rightarrow (-\Delta, -\tau, -G)$ and H unchanged.

Equation (14) may be handled in several ways. A variational analysis with the trial function $\psi_s = e^{-\lambda z^2/2}$ is found to reproduce the results of Ref. 1 [Eqs. (33), (37), and (39)] with the replacement $G + H \rightarrow \pi \hat{G}_0$. This replacement gives better agreement with numerical solutions of Eqs. (6a) and (6b) than the definition of \hat{G}_0 in Ref. 1. However, the variational results are still rather crude, and not accurate to more than a factor of two because $e^{-\lambda z^2/2}$ falls off much too rapidly to capture the contributions from the tail of the actual wave function for small τ . In this paper, we make a more careful analytical attempt to approximately solve the eigenvalue problem. Equation (14) may be cast into an equivalent Schrödinger equation

$$\psi'' - V\psi = 0 , \quad (15)$$

where $V = -(1 - \Delta)(G + H)\delta(z) + 1 - (\Delta - \tau z^2)^2 - \tau/(1 - \Delta + \tau z^2) + 3\tau^2 z^2/(1 - \Delta + \tau z^2)^2$ and $\psi(z) = \psi_s(1 - \Delta + \tau z^2)^{-1/2}$. Type 1 solutions generally have $-1 < \text{Re}(\Delta) < 0$. Consequently, $(G + H)$ produces a confining delta function potential at the origin with the mode evanescent for small finite z . Small τ causes the potential to decrease parabolically for small z , creating a pair of turning points.

With τ small, we can approximate $V \cong -(1 - \Delta)(G + H)\delta(z) + 1 - (\Delta - \tau z^2)^2 - \tau/(1 - \Delta)$ and further model this with a parabolic potential that preserves the turning point,

$$V = -(1 - \Delta)(G + H)\delta(z) + 1 - \Delta^2 - \frac{\tau}{(1 - \Delta)} - \beta z^2, \quad (16)$$

where $\beta = \tau\{[1 - \tau/(1 - \Delta)]^{1/2} - \Delta\}$. The potential of Eq. (16) converts Eq. (15) into a ‘driven’ form of the standard parabolic cylinder equation¹⁶

$$\psi'' + \left(\frac{1}{4}x^2 - \alpha\right)\psi = -(1 - \Delta)(G + H)\delta(x)2^{-1/2}\beta^{-1/4}\psi(0), \quad (17)$$

where $x^2 = 2\beta^{1/2}z^2$ and $\alpha = [1 - \Delta^2 - \tau/(1 - \Delta)]/2\beta^{1/2}$. Decaying solutions for large z^2 are given by $U(-\alpha, \pm x e^{i\pi/4})$ [see Ref. 16]. The dispersion relation is obtained by integrating Eq. (17) across the origin and substituting the appropriate forms of $U(-i\alpha, 0)$ and $U'(-i\alpha, 0)$.

We find

$$\frac{\Gamma(\frac{1}{4} - \frac{i\alpha}{2})}{\Gamma(\frac{3}{4} - \frac{i\alpha}{2})} \frac{1 - \Delta}{(-\beta)^{1/4}} (G + H) = 4. \quad (18)$$

Since $|\alpha| \gg 1$ for τ small, we can approximate

$$\frac{\Gamma(\frac{1}{4} - \frac{i\alpha}{2})}{\Gamma(\frac{3}{4} - \frac{i\alpha}{2})} = \left(\frac{2i}{\alpha}\right)^{1/2} (1 - ie^{-\pi\alpha}) \left[1 + \frac{1}{(4\alpha)^2} + \mathcal{O}(\alpha^{-4})\right], \quad (19)$$

by using two terms of Stirling’s formula. The dispersion relation may then be written

$$\Delta = -\frac{1 - p^2}{1 + p^2} + \frac{\tau}{(1 + p^2)(1 - \Delta)^2}, \quad (20)$$

where $p = (G + H)(1 - ie^{-\pi\alpha})[1 + 1/(4\alpha)^2]$. The exponential factor in p represents a non-perturbative contribution to the damping caused by components of the wave function that

propagate past the turning points toward infinity. These are KAW's. The non-perturbative damping may be thought of as tunnelling to the continuum, if one regards the propagating KAW's as a part of the MHD continuum. Real and imaginary parts of Eq. (20) are plotted as a function of $|\tau|$ in Fig. 1 for a particular case along with a direct numerical solution of Eqs. (6a) and (6b). Agreement is excellent up to $|\tau| \cong 0.5$. Quite significantly, the non-perturbative effects begin abruptly for the rather small value $|\tau| \cong 2 \times 10^{-3}$ for this choice of parameters. The analytic solution is no longer valid for $|\tau| > 0.5$ because the parabolic potential approximation breaks down.

For $\tau_i \ll \tau_r$ we can further simplify Eq. (20) as

$$\Delta_i = \frac{\tau_i}{2(1 - \Delta_0^2)} - (1 - \Delta_0^2) \exp \left[-\frac{\pi(1 - \Delta_0^2)}{2^{3/2} \tau^{1/2}} \right], \quad (21)$$

where $\Delta_0 \equiv -[1 - (G + H)^2/4]/[1 + (G + H)^2/4]$ represents the ideal ($\tau = 0$) eigenfrequency. The first term in Eq. (21) represents the correct form for the perturbative damping. [We point out that it is a factor of 2 larger than that given by Eq. (33) of Ref. 1. The discrepancy is due to the fact that the trial function $\psi_s = e^{-\lambda y^2/2}$ used in the variational calculation of Ref. 1 is not adequate for small τ . The correct perturbative form is recovered with the trial function $\psi_s = e^{-\lambda |y|/2}$.] The second term in Eq. (21) represents the non-perturbative component of the damping for small τ . Because of the way τ enters the exponential term, it is apparent that the non-perturbative effects can become significant for small values of τ , especially for Δ_0^2 near unity. In Fig. 1, $\Delta_0 = -0.776$. Equation (21) also agrees well with numerical results.

Type 2 solutions may be handled in a similar manner. With the replacements $(\Delta, \tau, G) \rightarrow (-\Delta, -\tau, -G)$ we can approximate

$$V \cong (1 + \Delta)(G - H)\delta(z) + 1 - \Delta^2 + \frac{\tau}{1 + \Delta} + \beta z^2, \quad (22)$$

where $\beta = \tau\{[1 + \tau/(1 + \Delta)]^{1/2} + \Delta\}$. Type 2 solutions generally have $0 < \text{Re}(\Delta) < 1$. Thus, the delta function potential at the origin is non-confining, and τ produces a confining

parabolic potential well for small finite z . Consequently, τ creates these modes. Now the alternative standard form of the parabolic cylinder equation applies,

$$\psi'' - \left(\frac{1}{4}x^2 + \alpha\right)\psi = (1 + \Delta)(G - H)\delta(x)2^{-1/2}\beta^{-1/4}\psi(0) , \quad (23)$$

where $x^2 = 2\beta^{1/2}z^2$, $\alpha = [1 - \Delta^2 + \tau/(1 + \Delta)]/2\beta^{1/2}$. Decaying solutions for large z^2 are given by $U(\alpha, \pm x)$. Integrating across the origin and substituting the appropriate forms of $U(\alpha, 0)$ and $U'(\alpha, 0)$ produces

$$\frac{\Gamma(\frac{1}{4} + \frac{\alpha}{2})}{\Gamma(\frac{3}{4} + \frac{\alpha}{2})} \frac{(1 + \Delta)}{\beta^{1/4}} (G - H) = -4 . \quad (24)$$

Since $\text{Re}(\alpha) \ll -1$ for small τ , we can approximate

$$\frac{\Gamma(\frac{1}{4} + \frac{\alpha}{2})}{\Gamma(\frac{3}{4} + \frac{\alpha}{2})} = \left(\frac{2}{-\alpha}\right)^{1/2} \cot\left(\frac{1}{4} + \frac{\alpha}{2}\right) \left[1 - \frac{1}{(4\alpha)^2} + \mathcal{O}(\alpha^{-4})\right] , \quad (25)$$

by using the reflection formula for the gamma functions and then two terms from Stirling's formula. The dispersion relation takes on a completely different form,

$$\Delta = \left[1 + \frac{\tau}{1 + \Delta}\right]^{1/2} + \frac{\tau^{1/2}\{1 + 4\ell + \frac{4}{\pi} \arctan [(G - H)(1 + \Delta)^{1/2}/2^{3/2}]\}}{\{\Delta + [1 + \tau/(1 + \Delta)]^{1/2}\}^{1/2}} , \quad (26)$$

where ℓ is a non-negative integer. The countable infinity of modes are associated with the poles in the gamma functions for negative argument. These modes represent the kinetic EAE (KEAE) or kinetic TAE (KTAE). As discussed in Ref. 1, they are caused by the coupling of two propagating KAW in the gap region. For $\ell = 0$ and $(G - H) = 0$, Eq. (26) reduces to the dispersion relation Eq. (39) of Ref. 1, obtained by variational techniques. The damping $\Delta_i \sim \tau_i/\sqrt{\tau_r}$. The MHD boundary condition $(G - H)$ enters through the argument of the arctangent and gives a correction of $\mathcal{O}(1)$. Real and imaginary parts of Eq. (26) are plotted as a function of $|\tau|$ in Fig. 2 for a particular case along with a direct numerical solution of Eqs. (6a) and (6b). Agreement is excellent up to $|\tau| \cong 0.1$. [Better agreement is obtained for larger $\text{Arg}(\tau)$.] For $|\tau| > 0.1$, the parabolic potential approximation breaks down and

tunnelling, due to the quartic component of the potential, begins. We remark that Eq. (26) gives only Type 2 KT/EAE. There are also Type 1 KT/EAE, which obey a dispersion relation similar to Eq. (26) with $\ell = 1/2, 3/2, \dots$. However, $\ell = 0$ is the least damped, and therefore the most interesting, KT/EAE.

IV. The Parameter τ

Kinetic effects on the T/EAE's are determined by the magnitude of the parameter τ . For the TAE, this parameter reads

$$\tau = \frac{8s^2}{(2r/R)^3} \left(\frac{\rho_s}{r} \right)^2 (m_1 m_2)^{1/2} (m_1 + m_2) F^{-1}, \quad (27)$$

while for the EAE, it reads

$$\tau = \frac{2s^2}{(\chi - 1)^3} \left(\frac{\rho_s}{r} \right)^2 (m_1 m_2)^{1/2} (m_1 + m_2) F^{-1}, \quad (28)$$

where χ represents the elongation of the plasma. Therefore, for the EAE, this parameter is a factor of $2\{r/[R(\chi - 1)]\}^3$ times that for the TAE. For DIII-D this factor is approximately $0.25(r/r_p)^3$ times smaller. Thus, for elongated plasmas, kinetic effects become important for higher EAE mode numbers, e.g. $m = 4$ or 5 rather than 1 or 2 , which is the case for TAE. However, since the growth rate for the EAE is also reduced by an order of magnitude because of the higher frequency and effective wavenumber, the lower damping is mitigated by lower growth.

V. Conclusions

We have extended the non-perturbative kinetic analysis of the TAE to the EAE. Since 'ellipticity' for an elongated plasma like DIII-D is larger than the effective toroidicity, the kinetic effects are in general weaker for EAE than they are for TAE. The parameter that measures the kinetic character (of the EAE) is rather small for lower mode numbers, but

can be of order unity or larger for higher mode numbers; the parameter scales as the square of the mode number. While the lower mode number EAE's therefore have a strongly MHD character, they do not necessarily have a perturbatively small damping. This is because, quite significantly, the transition to the non-perturbative regime can begin for fairly small values of the kinetic parameter. In the non-perturbative regime, the damping is enhanced because the KAW carries the mode energy away from the gap region. Naturally, the damping in this regime is quite insensitive to the details of the dissipation mechanism. In addition to altering the mode structure of this basically MHD mode, kinetic effects introduce a countable infinity of new modes, formed by the coupling between two KAW's. These kinetic T/EAE (KT/EAE) have eigenfrequencies which lie just above the gap. The lowest KT/EAE may actually have a lower damping rate than the corresponding T/EAE due to non-perturbative effects. This makes the KT/EAE potentially more important than the T/EAE under some conditions: strong shear, high temperature, and moderate mode numbers.

Acknowledgments

One of us, R.R.M., is grateful to H.L. Berk for helpful discussions and criticisms. This work is funded in part by the U.S. Department of Energy Contract No. DE-FG05-80ET53088.

References

1. R.R. Mett and S.M. Mahajan, Phys. Fluids B **4**, 2885 (1992).
2. C.Z. Cheng and M.S. Chance, Phys. Fluids **29**, 3695 (1986).
3. G.Y. Fu and J.W. Van Dam, Phys. Fluids B **1**, 1949 (1989).
4. C.Z. Cheng, Phys. Fluids B **3**, 2463 (1991).
5. R. Betti and J.P. Freidberg, Phys. Fluids B **3**, 1865 (1991).
6. K.L. Wong *et al.*, Phys. Rev. Lett. **66**, 1874 (1991).
7. W.W. Heidbrink, E.J. Strait, E. Doyle, G. Sager, and R.T. Snider, Nuc. Fusion **31**, 1635 (1991).
8. F. Zonca and L. Chen, Phys. Rev. Lett. **68**, 592 (1992).
9. M.N. Rosenbluth, H.L. Berk, J.W. Van Dam, and D.M. Lindberg, Phys. Rev. Lett. **68**, 596 (1992).
10. M.N. Rosenbluth, H.L. Berk, J.W. Van Dam, and D.M. Lindberg, Phys. Fluids B **4**, 2189 (1992).
11. H.L. Berk, J.W. Van Dam, Z. Guo, and D.M. Lindberg, Phys. Fluids B **4**, 1806 (1992).
12. N.N. Gorelenkov and S.E. Sharapov, Physica Scripta **45**, 163 (1992).
13. R.D. Hazeltine and J.D. Meiss, Phys. Reports **121**, 1 (1985).
14. A. Hasegawa and L. Chen, Phys. Rev. Lett. **35**, 370 (1975).
15. S.M. Mahajan, Phys. Fluids **27**, 2238 (1984).

16. M. Abramowitz and I.A. Stegun, eds., *Handbook of mathematical functions with formulas, graphs, and mathematical tables*, (National Bureau of Standards Applied Mathematics Series 55, Washington, D.C., 1964).

Figure Captions

1. T/EAE: Comparison of analytic dispersion relation, Eq. (20), with numerical shooting code results. Solid lines indicate real part and dashed lines the negative imaginary part of $(\Delta + 1)$ vs. $|\tau|$. The label “C” designates numerical solution of Eqs. (6a) and (6b) while the unlabeled curves correspond to Eq. (20). Here, $\hat{\varepsilon} = 0.117$, $\hat{G}_1 = 1.378$, $\hat{G}_2 = -0.351$, $\psi_1 = 0.710$, $\psi_2 = 1.412$.
2. KT/EAE: Comparison of analytic dispersion relation, Eq. (26), with numerical shooting code results. Solid lines indicate real part and dashed lines the negative imaginary part of $(\Delta + 1)$ vs. $|\tau|$. The label “C” designates numerical solution of Eqs. (6a) and (6b) while the unlabeled curves correspond to Eq. (26). Here, $\hat{\varepsilon} = 0.117$, $\hat{G}_1 = 1.378$, $\hat{G}_2 = -0.351$, $\psi_1 = 0.710$, $\psi_2 = 1.412$.

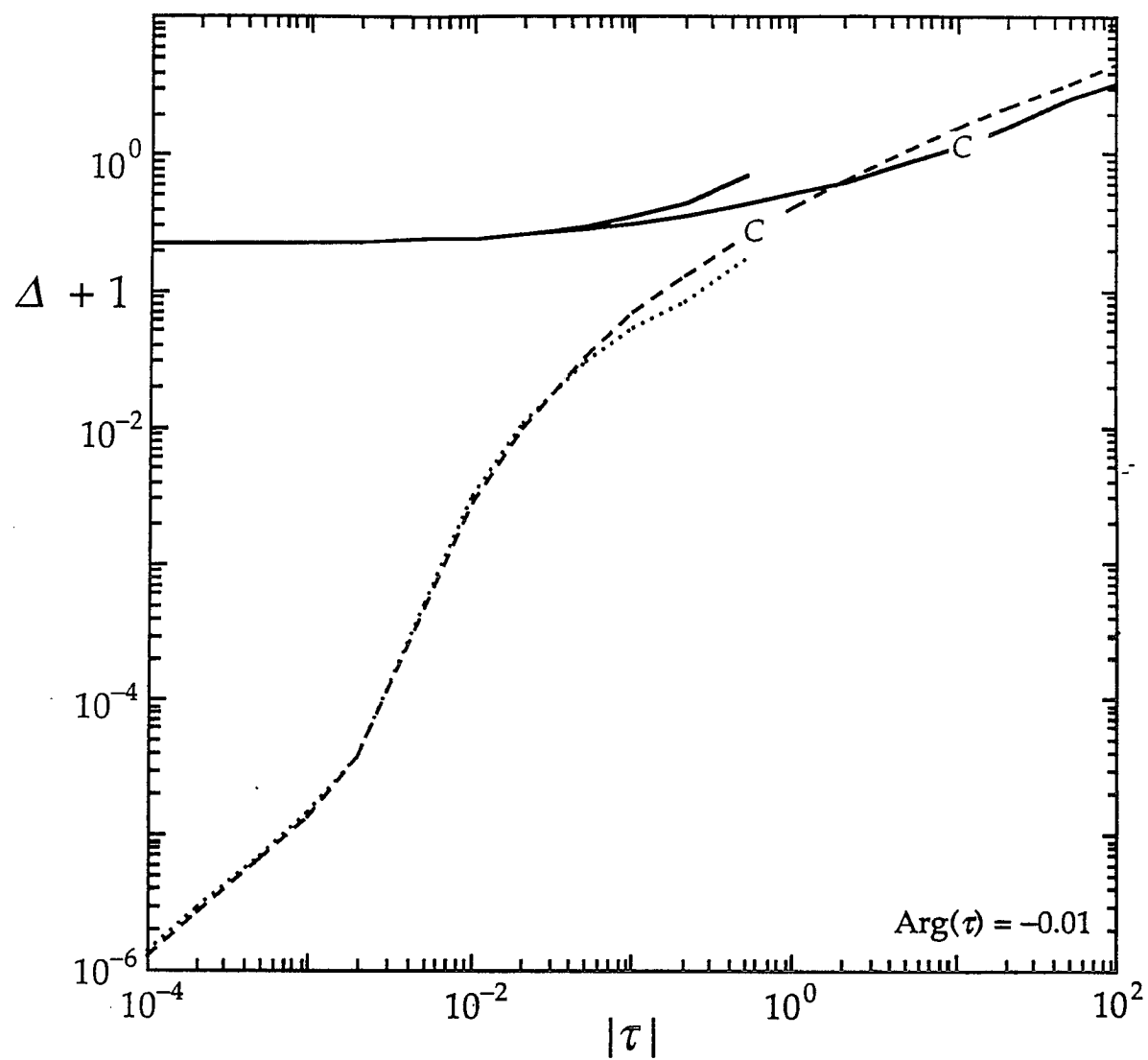


Fig. 1

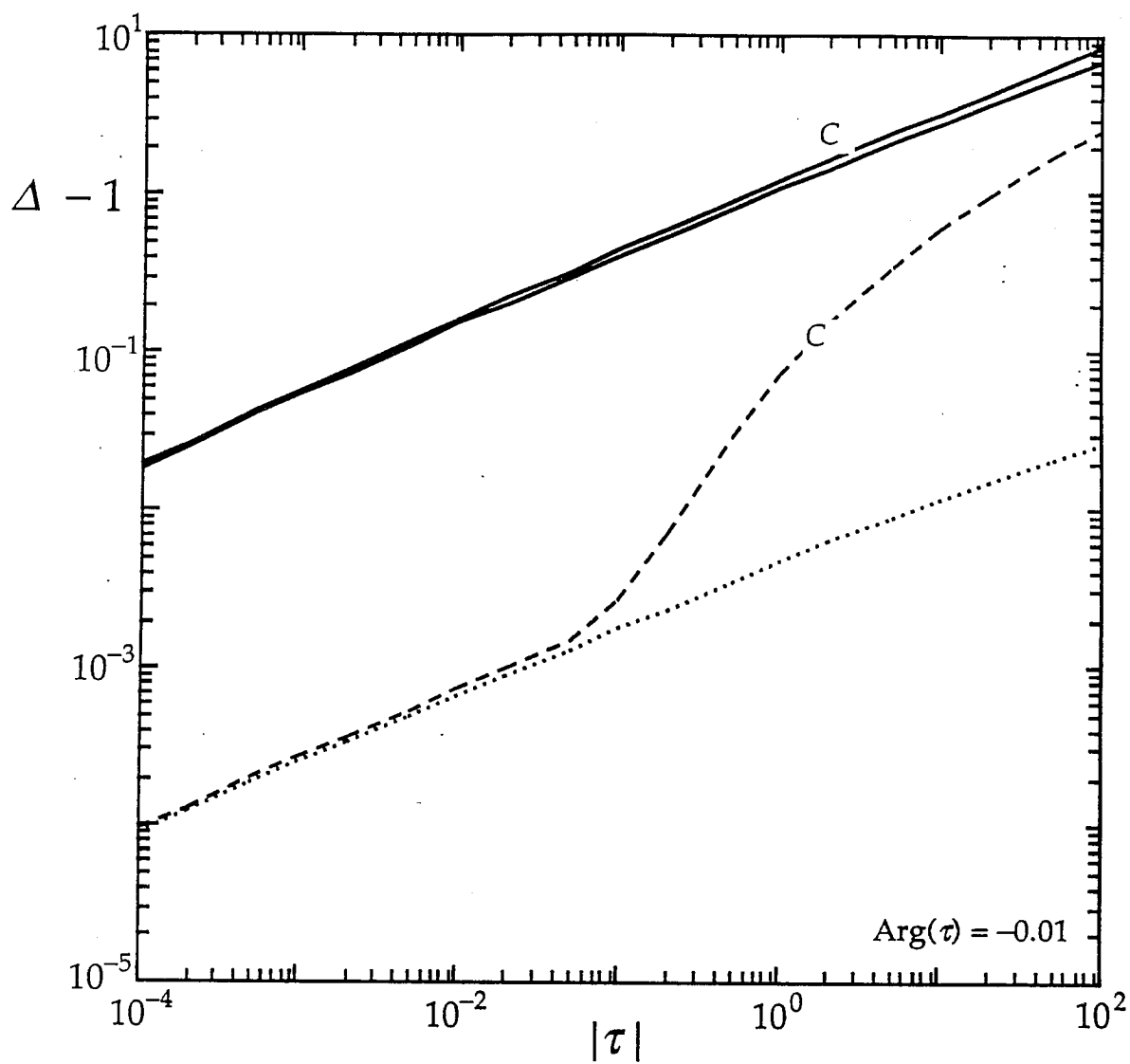


Fig. 2

